Differentiation in additive and multiplicative inputs to motoneuron pool as origins of spasticity – a neuromorphic modeling study*

Zhi Chen, Yang Liu, Jin Yan, Jixian Wang, Denny Oetomo,

Ying Tan and Chuanxin M.Niu*

***Abstract*—Spasticity is characterized by a velocity-dependent increase in the tonic stretch reflex. Evidence suggests that spasticity originates from hyperactivity in the descending tract or reflex loop. To pinpoint the source of hyperactivity, however, is difficult due to lack of human data in-vivo. Thus, we implemented a neuromorphic model to revive the neuro-dynamics with spiking neuronal activity. Two types of input were modeled: (1) the additive condition (ADD) to apply tonic synaptic inputs directly into the reflex loop; (2) the multiplicative (MUL) condition to adjust the loop gains within the reflex loop. Results show that both conditions produced antagonist EMG responses resembling patient data. The timing of spasticity is more sensitive to the ADD condition, whereas the amplitude of spastic EMG is more sensitive to the MUL condition. In conclusion, our model shows that both additive and multiplicative hyperactivities suffice to elicit velocity-dependent spastic electromyographic signals (EMG), but with different sensitivities. This simulation study suggests that spasticity caused by different origins may be discernable by the progression of severity, which may help individualized goal-setting and parameter-selection in rehabilitation.**

***Clinical Relevance*—Potential application of neuromorphic modeling on spasticity includes selection of parameters for therapeutic plans, such as movement range, repetition, and load.**

I. Introduction

Spasticity is a condition characterized by a velocity-dependent increase in additive stretch reflexes[1], which present in about 20%-40% stroke survivors [2]. Evidence suggests that two types of hyperactivities may account for spasticity: (1) additive (ADD), e.g., the increased synaptic input due to the imbalanced descending tract or decreased inhibitory inputs to the motoneuron pool [3]; (2) multiplicative (MUL), e.g., the increased loop gain due to the persistence inward current [4], over-release of neurotransmitter, or intrinsic neuron changes [5]. However, the links between two hyperactivities and the corresponding clinical symptoms (mainly EMG) remain unclear due to the difficulty in the acquisition of human data.

The origin of spasticity is likely associated with an unbalanced control of spinal reflexes at the supraspinal level (e.g., cortical injury). Previous studies reported hyperexcitability in the vestibulospinal tract [6], damage to pyramidal neurons [7], and loss of inhibitory effects in segmental reflexes [8] in spastic patients. Researchers have assumed that lesions in the motor-related cortex or internal capsule reduce the inputs of the contralateral dorsal reticulospinal tract [3], which in turn facilitates the medial reticulospinal tract and vestibulospinal tract, leading to hyperexcitable spinal reflex [9].

Abnormalities at the spinal and peripheral level (e.g., the gain of the stretch reflex loop) also contribute to spasticity. Spasticity may arise from several sources: (1) increased sensitivity of muscle spindles through γ motor system [10]; (2) enhanced responses to muscle afferent input due to collateral sprouting [11] and denervation hypersensitivity [12]; and (3) changes in intrinsic electrical properties of neurons [5]. However, these experiments were conducted on anesthetized animals or applied chemical destruction, neither of which can be applied to spastic patients.

Bio-realistic simulation has been proposed to explore the mechanisms of several symptoms. It has been suggested that loop delay combined with hyperexcitation in motoneuron pools triggers clonus [13]. However, previous models did not capture the spiking behaviors of neurons. As suggested by the information theory [14], the function of neuron is to converted post-synaptic currents into a train of binary spikes with limited bandwidth. In other words, a neuron should be modeled to satisfy the protocol of "current-in, spike-out" if the neuromorphic model focuses on its functional role. Moreover, spike-based models generate EMG signals that can be verified against human data.

Neuromorphic models enabled the multi-scale tracing of neural activity detailed from neuron spikes. Using a spike-based model, we examined two kinds of hyperactivity around the spinal reflex loop, and their capability to incur spasticity. We are particularly interested in whether the ADD and MUL conditions show any difference while producing spastic EMGs in response to limb stretch.

*Research supported by the National Natural Science Foundation of China (81971722); Shanghai Science and Technology Commission Project (22490711000); A grant of the National Key R&D Program of China by the Ministry of Science and Technology of China (No. 2017YFA0701103).

Z.C, Y.L., J.Y, J.W., and C.M.N., are with the Department of Rehabilitation Medicine, Ruijin Hospital, Shanghai Jiao Tong University School of Medicine, Shanghai, China, 200025 (corresponding author: Chuanxin M. Niu, e-mail: minos.niu@ gmail.com).

D.O. and Y.T. are with the University of Melbourne and Fourier Intelligence Joint Laboratory, Faculty of Engineering and IT, The University of Melbourne, Parkville, VIC, Australia.

II. METHODS

A. Model of monosynaptic reflex loop

The simulated reflex loop is a monosynaptic spinal reflex consisting of one antagonist, the muscle spindles, sensory neuron pools, synapses, and motoneuron pools, as shown in FIG.1. The major difference between our model and previous models on spasticity [13] is the inclusion of spiking neurons following the Izhikevich model [15], which allows for the reviving of the spiking dynamic of neurons. The software

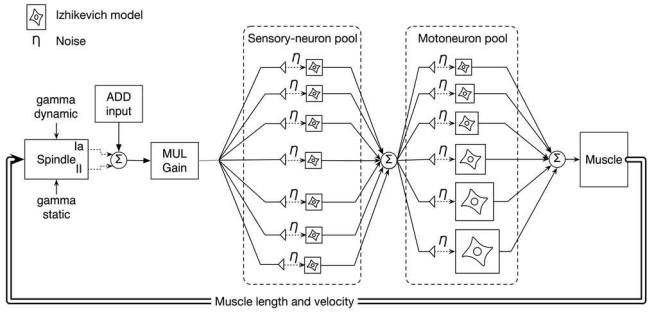

Figure 1. The system architecture: A total of 40 spiking neurons (20 sensory neurons, 20 motor neurons) were simulated. The ADD condition is implemented by adding tonic input that is independent of the sensory feedback. The MUL condition is implemented by increasing the loop gain of the spindle afferents. Nosie is a uniformly distributed random signal ranging from -0.1 to 0.1.

implementation of the model included 40 spiking neurons. We have also created a hardware implementation using a neuromorphic architecture [16] on a FPGA chip (Anlogic, SF1 FPSoC, Shanghai, China), which successfully emulated 3,072 spiking neurons at 1000 Hz sampling rate.

The following events occurred when the muscle was stretched: (1) the stretch length was input to muscle spindles to generate afferent current; (2) afferent current activated a train of sensory neurons; (3) the synapses transferred sensory neurons spikes into current; (4) the current activated a train of motoneurons; (5) the motoneuron spikes activated a muscle model; (6) the muscle model computed EMG signals. The models of muscle spindles, sensory neuron pools and synapses have been reported in our previous studies [16].

B. Stretch responses and sensitivity analyses

Three simulation experiments were conducted. The stretch simulations were represented by the displacement profiles of muscle, which were calculated using minimal-jerk formulation [17]:

$$x(t) = x_i + (x_f - x_i)(10\left(\frac{t}{d}\right)^3 - 15\left(\frac{t}{d}\right)^4 + 6\left(\frac{t}{d}\right)^5) \quad (1)$$

Here $x(t)$ represents the position trajectory in one dimension. x_i is the starting position, x_f is the ending position, and t is the movement duration.

The severity of spasticity was measured in timing metric and amplitude metric. The timing metric of spasticity was represented by the center point of EMG responses using the following equations:

$$\sum_{onset}^{center} EMG = \frac{1}{2}\sum_{onset}^{t} EMG \quad (2)$$

Where t is the movement duration, $onset$ is the position where the EMG burst higher than the threshold for the first time. The severity of spasticity was assessed using polynomial fitting:

$$duration = \beta_0 + \beta_1 x_i \ \ (i = 1,2,\dots,7) \quad (3)$$

Where i is the number of stretch experiments, x_i represents the center of EMG responses of ith stretch. β_0 and β_1 are the fitting parameters. In our study, we refer to β_1 as a measure of severity for spasticity.

The amplitude metric was represented by the peak value of EMG responses. The higher the peak EMG, the worse the spasticity.

In simulation 1, the antagonist was stretched at 7 different speeds [18] to investigate the impact of both conditions on the timing metrics of spasticity.

In simulation 2, the antagonist was stretched at 1 fixed speed to investigate the impact of both conditions on the amplitude metrics of spasticity.

In simulation 3, the antagonist was stretched at various speeds with 2 fixed condition parameters (ADD and MUL respectively) to test whether spastic EMG caused by 2 conditions can be differentiated.

During the validation of each simulation, the simulated EMG of the skeletal muscle stayed silent with a baseline condition, but it started showing clear EMG bursts with excessive input superimposed to the baseline. The simulations ended when the EMG responses stopped changing significantly, mainly due to the saturation of neurons.

C. Signal processing and statistics

All data were sampled at 1024Hz. The EMG signals were high-pass filtered at 5Hz, rectified and low-pass filtered at 20Hz cut-off frequency. All procedures were performed using MATLAB 2020b (Math works, Inc.).

D. Statistical analysis

We ran a linear regression model to differentiate ADD and MUL conditions using the following equation:

$$severity \sim parameter + type + parameter * type \quad (10)$$

Where $severity$ was either measured by timing or amplitude, $parameter$ represents the normalized condition parameters, $type$ represents the condition type, either MUL or ADD condition. The significant level was set to 0.05.

III. RESULTS

A. Both conditions produced spastic EMG patterns

We first examined the simulated EMG responses. As shown in Figure.3, the baseline produced no EMG responses to the stretches. When the excessive inputs from ADD and MUL conditions were added, both models produce antagonist EMG responses compatible with human data [19].

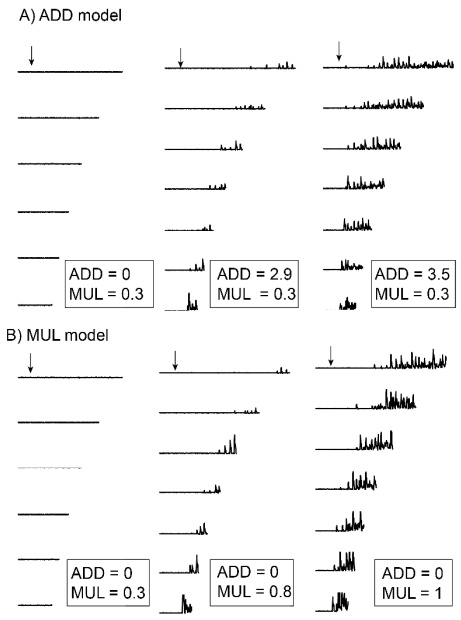

Figure 2. Both ADD and MUL conditions are suffice to generate spastic EMG signals. The simulated EMG stayed silent with a baseline condition, and it started showing clear EMG bursts with excessive input. (A) The simulation results of ADD condition, the higher the inputs, the more sever the spasticity. (B) The simulation results of MUL condition, the higher the MUL gain, the more sever the spasticity.

B. *Simulation 1: the timing of severity is more sensitive to ADD condition*

In simulation 1, the muscle was stretched with 7 different speeds. The severities of spasticity were measured using timing metric – the center of EMG responses. The higher the severity, the sooner the center appears. As shown in Figure.3, the severity of spasticity significantly correlates with ADD parameters (slope = 1.0978, $p < 0.00001$, $r^2 = 0.7989$) and MUL parameters (slope = 0.4447, $p < 0.000001$, $r^2 = 0.9404$). The significantly interactive effect is also observed ($p < 0.0001$). MUL condition shows stronger linear trend than add condition, but the severity is more sensitive to ADD condition.

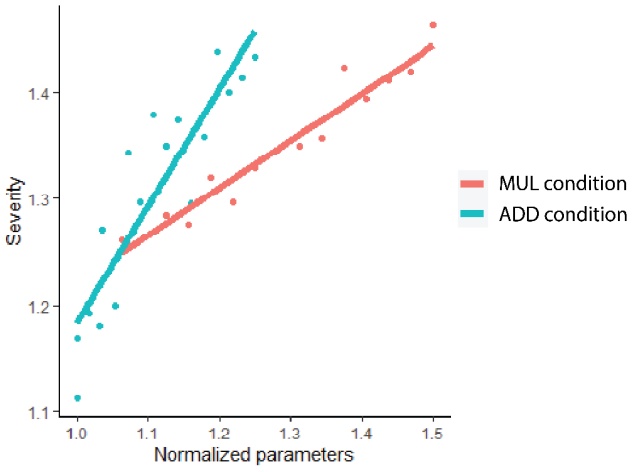

Figure 3. Simulation 1. The severity of spasticity was measured by the timing metric, higher severity means the earlier burst of EMG responses center. The severity of spasticity measured in timing metric was more sensitive to ADD condition than MUL condition.

C. *Simulation 2: the MUL condition produced wider range of EMG magnitude*

In simulation 2, the muscle was stretched at one fixed speed. The baseline and end of simulation are shown in Figure.4A. The simulations ended when the neurons saturated. As shown in Figure.4B, the peak EMG responses of ADD condition range from 0 to 135, while the peak responses of MUL condition range from 0 to 325. The upper limit of MUL condition is 241% higher than ADD condition.

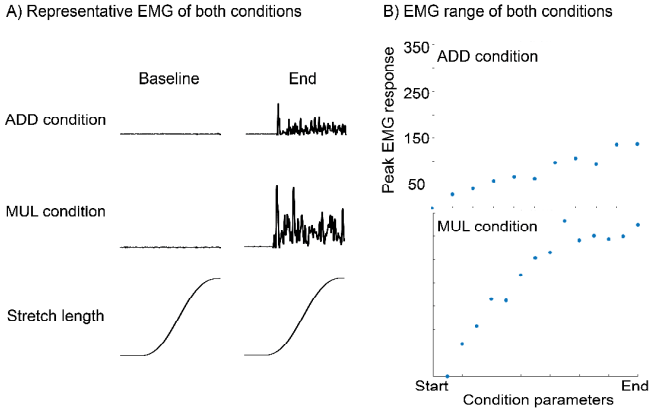

Figure 4. Simulation 2. The parameters were added progressively from baseline to quantify the possible clinical outcomes. (A) the start and end of simulation. The simulations were terminated when the neurons burst at the resting current (the end). B) the range of peak EMG responses of both conditions.

D. *Simulation 3: the MUL condition differs from the ADD condition under high stretch speed*

In simulation 3, 2 spastic muscles were corrected using ADD and MUL condition respectively, and were stretched at various speeds. As shown is Figure.5, in low-speed situations, both conditions show similar EMG responses. When the stretch speed is relatively high (i.e., stretch duration lower than 2500 sample points), MUL condition rises higher and quicker than ADD condition.

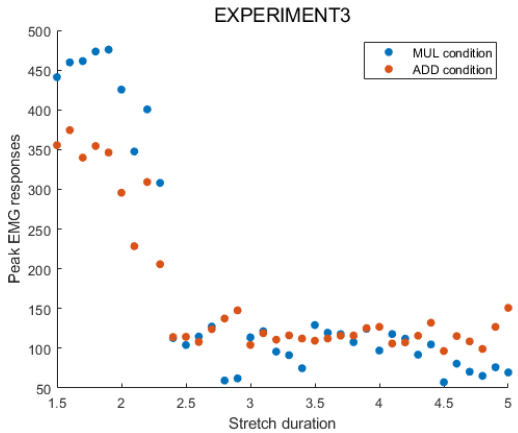

Figure 5.Simulation 3. Two typical spastic conditions were created using ADD and MUL parameters and stretched at various speeds to quantify the peak EMG responses. When the velocities are

relatively high, the EMG responses of MUL condition rise higher and quicker than ADD condition.

IV. Discussion

We compared 2 types of hyperactivities with monosynaptic reflex circuitry using neuromorphic simulation. Results show that both additive synaptic inputs and multiplicative loop gain sufficed to trigger EMG responses resembling patient data. Simulated spastic EMGs exhibit distinct EMG responses. In short, the timing of spastic EMG was more sensitive to additive inputs, while the amplitude spastic EMG was more sensitive to multiplicative loop gain.

This simulation study suggests that spasticity caused by different origins may have distinct EMG features, which may help individualized goal-setting and parameter-selection in rehabilitation. the treatment of spasticity acts on different mechanisms: the pharmacotherapy mainly acts on the MUL mechanism, the drugs reduce the release of neurotransmitters (e.g., Baclofen), while the rehabilitation therapy acts on the ADD mechanism (e.g., rebalance the cortical inhibition using TMS). Differentiation between different origins of spasticity may guide the treatment plans and maximize the therapeutic effects.

Compared to experimental studies of spasticity, our modeling approach allows "virtual conditioning" of reflex pathways with physiologically justifiable parameters. Several limitations do exist with the current model: first, the simulation ignored certain physiological details (e.g., the reciprocal inhibition process). Second, the dichotomy of ADD and MUL conditions are agnostic about supra-spinal abnormalities. Our model reserved the flexibility of adding these details.

V. Conclusion

This simulation study shows that both increased additive synaptic inputs and loop gain could produce spasticity. However, the timing metric of spasticity is more sensitive to the ADD condition, while the MUL condition incurs wider range of EMG responses. Our results suggest a new rationale for sub-categorization of spasticity tailored to neuronal abnormalities.

References

[1] J. W. Lance, "Symposium synopsis," *Spasticity Disord. Mot. Control*, 1980.

[2] R. D. Zorowitz, P. J. Gillard, and M. Brainin, "Poststroke spasticity: Sequelae and burden on stroke survivors and caregivers," *Neurology*, vol. 80, no. Issue 3, Supplement 2, pp. S45–S52, Jan. 2013, doi: 10.1212/WNL.0b013e3182764c86.

[3] S. Li, Y.-T. Chen, G. E. Francisco, P. Zhou, and W. Z. Rymer, "A Unifying Pathophysiological Account for Post-stroke Spasticity and Disordered Motor Control," *Front. Neurol.*, vol. 10, p. 468, May 2019, doi: 10.3389/fneur.2019.00468.

[4] J. G. McPherson, M. D. Ellis, C. J. Heckman, and J. P. A. Dewald, "Evidence for Increased Activation of Persistent Inward Currents in Individuals With Chronic Hemiparetic Stroke," *J. Neurophysiol.*, vol. 100, no. 6, pp. 3236–3243, Dec. 2008, doi: 10.1152/jn.90563.2008.

[5] D. Burke, J. Wissel, and G. A. Donnan, "Pathophysiology of spasticity in stroke," *Neurology*, vol. 80, no. Issue 3, Supplement 2, pp. S20–S26, Jan. 2013, doi: 10.1212/WNL.0b013e31827624a7.

[6] D. M. Miller, C. S. Klein, N. L. Suresh, and W. Z. Rymer, "Asymmetries in vestibular evoked myogenic potentials in chronic stroke survivors with spastic hypertonia: Evidence for a vestibulospinal role," *Clin. Neurophysiol.*, vol. 125, no. 10, pp. 2070–2078, Oct. 2014, doi: 10.1016/j.clinph.2014.01.035.

[7] R. Bhimani and L. Anderson, "Clinical Understanding of Spasticity: Implications for Practice," *Rehabil. Res. Pract.*, vol. 2014, pp. 1–10, 2014, doi: 10.1155/2014/279175.

[8] D. Burke and P. Ashby, "Are spinal 'presynaptic' inhibitory mechanisms suppressed in spasticity?," *J. Neurol. Sci.*, vol. 15, no. 3, pp. 321–326, Mar. 1972, doi: 10.1016/0022-510X(72)90073-1.

[9] P. Brown, "Pathophysiology of spasticity.," *J. Neurol. Neurosurg. Psychiatry*, vol. 57, no. 7, pp. 773–777, Jul. 1994, doi: 10.1136/jnnp.57.7.773.

[10] P. Dietrichson, "PHASIC ANKLE REFLEX IN SPASTICITY AND PARKINSONIAN RIGIDITY," *Acta Neurol. Scand.*, vol. 47, no. 1, pp. 22–51, Mar. 1971, doi: 10.1111/j.1600-0404.1971.tb07462.x.

[11] D. Lemaitre and F. Court, "New insights on the molecular mechanisms of collateral sprouting after peripheral nerve injury," *Neural Regen. Res.*, vol. 16, no. 9, p. 1760, 2021, doi: 10.4103/1673-5374.306069.

[12] L.-G. Nygren and L. Olson, "On spinal noradrenaline receptor supersensitivity: Correlation between nerve terminal densities and flexor reflexes various times after intracisternal 6-hydroxydopamine," *Brain Res.*, vol. 116, no. 3, pp. 455–470, Nov. 1976, doi: 10.1016/0006-8993(76)90493-5.

[13] J. M. Hidler and W. Z. Rymer, "A simulation study of reflex instability in spasticity: origins of clonus," *IEEE Trans. Rehabil. Eng.*, vol. 7, no. 3, pp. 327–340, Sep. 1999, doi: 10.1109/86.788469.

[14] T. D. Sanger, "Distributed Control of Uncertain Systems Using Superpositions of Linear Operators," *Neural Comput.*, vol. 23, no. 8, pp. 1911–1934, Aug. 2011, doi: 10.1162/NECO_a_00151.

[15] E. M. Izhikevich, "Simple model of spiking neurons," *IEEE Trans. Neural Netw.*, vol. 14, no. 6, pp. 1569–1572, Nov. 2003, doi: 10.1109/TNN.2003.820440.

[16] C. M. Niu, K. Jalaleddini, W. J. Sohn, J. Rocamora, T. D. Sanger, and F. J. Valero-Cuevas, "Neuromorphic meets neuromechanics, part I: the methodology and implementation," *J. Neural Eng.*, vol. 14, no. 2, p. 025001, Apr. 2017, doi: 10.1088/1741-2552/aa593c.

[17] T. Flash and N. Hogan, "The coordination of arm movements: an experimentally confirmed mathematical model," *J. Neurosci.*, vol. 5, no. 7, pp. 1688–1703, Jul. 1985, doi: 10.1523/JNEUROSCI.05-07-01688.1985.

[18] X. Guo, R. Wallace, Y. Tan, D. Oetomo, M. Klaic, and V. Crocher, "Technology-assisted assessment of spasticity: a systematic review," *J. NeuroEngineering Rehabil.*, vol. 19, no. 1, p. 138, Dec. 2022, doi: 10.1186/s12984-022-01115-2.

[19] M. F. Levin and A. G. Feldman, "The role of stretch reflex threshold regulation in normal and impaired motor control," *Brain Res.*, vol. 657, no. 1–2, pp. 23–30, Sep. 1994, doi: 10.1016/0006-8993(94)90949-0.